Preprints (www.preprints.org) | NOT PEER-REVIEWED | Posted: 5 April 2021 doi:10.20944/preprints202104.0112.v1

Article

Dynamical localization simulated on actual quantum hardware

Andrea Pizzamiglio[1], Su Yeon Chang[2,3], Maria Bondani[4], Simone Montangero[5,6,7], Dario Gerace[8], and Giuliano Benenti [1,9,10,*]

1 Dipartimento di Scienza e Alta Tecnologia, Università degli Studi dell'Insubria, via Valleggio 11, 22100 Como, Italy
2 Institute of Physics, Ecole Polytechnique Fédérale de Lausanne (EPFL), 1015 Lausanne, Switzerland
3 CERN, 1211 Meyrin, Switzerland
4 Istituto di Fotonica e Nanotecnologie, Consiglio Nazionale delle Ricerche, via Valleggio 11, 22100 Como, Italy
5 Dipartimento di Fisica e Astronomia "G. Galilei," Università di Padova, 35131 Padova, Italy
6 Istituto Nazionale di Fisica Nucleare, Sezione di Padova, 35131 Padova, Italy
7 Padua Quantum Technology Research Center, Università di Padova, I-35131 Padova, Italy
8 Dipartimento di Fisica, Università di Pavia, via Bassi 6, 27100 Pavia, Italy
9 Istituto Nazionale di Fisica Nucleare, Sezione di Milano, via Celoria 16, 20133 Milano, Italy
10 NEST, Istituto Nanoscienze-CNR, I-56126 Pisa, Italy
* Correspondence: giuliano.benenti@uninsubria.it

Version March 31, 2021 submitted to Entropy

Abstract: Quantum computers are invaluable tools to explore the properties of complex quantum systems. We show that dynamical localization of the quantum sawtooth map, a highly sensitive quantum coherent phenomenon, can be simulated on actual, small-scale quantum processors. Our results demonstrate that quantum computing of dynamical localization may become a convenient tool for evaluating advances in quantum hardware performances.

Keywords: digital quantum simulation; quantum algorithms; quantum complex systems

1. Introduction

The simulation of complex systems is expected to be one of the main applications of future quantum computers [1]. The special role of quantum mechanics in simulation was pointed out long time ago by Feynman [2]. He observed that, while in a classical computer the memory requirements for the simulation of a many-body quantum system can grow exponentially with the number of particles, the growth is only polynomial in a quantum computer, which is itself a many-body quantum system. Lloyd [3] then validated the conjecture of an exponential speedup in the simulation of quantum systems by means of a quantum computer, with respect to a classical computer. Applications have been discussed for many physical models, so far (see, e.g., Refs. [4–13], and references therein). An ideal quantum computer operating with more than fifty qubits could outperform a classical computer, and the quantum advantage for specific problems has been recently claimed [14,15]. However, quantum advantage can only be reached with a high enough quantum gate precision and through processes generating a large enough amount of entanglement, otherwise they can be efficiently simulated via tensor network methods [16]. On the other hand, present-day quantum computers suffer from significant decoherence and the effects of various noise sources, such that the amount of entanglement that can be reached is still limited. Therefore, achieving the quantum advantage in complex, practically relevant problems such as chemical reactions, new materials design, or biological processes, is still an

© 2021 by the author(s). Distributed under a Creative Commons CC BY license.

Preprints (www.preprints.org) | NOT PEER-REVIEWED | Posted: 5 April 2021 doi:10.20944/preprints202104.0112.v1

imposing challenge. It is then important to benchmark the progress of currently available quantum computers by simulating less demanding but still physically significant tasks.

Dynamical localization is one of the most interesting phenomena that characterize the quantum behavior of classically chaotic systems: quantum interference effects suppress the diffusion taking place in the underlying classical model, leading to exponentially localized wave functions. This phenomenon, first discovered in the quantum kicked-rotor model [17,18], has been observed experimentally in the microwave ionization of Rydberg atoms [19], in atom-optic systems [20–22], and in nuclear magnetic resonance quantum ensemble computation [23]. Dynamical localization has deep analogies with Anderson localization of electronic transport in disordered materials [24]. Localization is indeed ubiquitous in wave physics, since it originates from the interference between multiple scattering paths. It has been shown that in a quantum computer simulating dynamical localization the amount of entanglement is deeply connected with the localization length of the system simulated [25].

In this paper, we simulate dynamical localization with three qubits by means of several IBM quantum processors, with the aim of analyzing the performances of currently available, noisy quantum hardware, freely available for cloud quantum computing. In particular, we use the known quantum algorithm for the quantum sawtooth map [26,27], which is the ideal model to investigate dynamical localization, and more generally quantum chaotic dynamics on a quantum computer. This is because all of the qubits are actually used to simulate dynamics, without the need for auxiliary qubits. Moreover, the quantum algorithm performs forward-backward Fourier transform, thus exploring the entire Hilbert space of the quantum register in a complex multiple-path interferometer that leads to wave-function localization. As such, dynamical localization is a very fragile quantum phenomenon, extremely sensitive to noise. Its effective simulation on an actual quantum hardware is therefore a potentially ideal test bench to illustrate the power of quantum computation.

Here we show that it is possible to detect quantum localization with $n = 3$ qubits and a single step of the sawtooth map, requiring $4n = 12$ single-qubit and $2(n^2 - n) = 12$ two-qubit quantum gates. We find that the height of the localization peak is smaller than the value expected for a noiseless quantum computer. Moreover, the peak reduction in real quantum processors is significantly larger than expected from the simulator provided by IBM, which only takes into account a limited number of noise channels. Our results show that for the best performing and freely available IBM quantum processors the localization peak does emerge from noise for about 3 map steps.

The paper is organized as follows. In Sec. 2 we describe the quantum algorithm for simulating dynamical localization, in Sec. 3 results obtained from IBM quantum processors are shown and compared with those from the IBM simulator and with the exact, noiseless evolution. Our conclusion are drawn in Sec. 4.

2. Quantum algorithm for the dynamical localization

2.1. Quantum algorithm for the sawtooth map

The most convenient model to simulate dynamical localization on a quantum computer is the quantum sawtooth map. This map describes the dynamics of a periodically driven system, as derived from the Hamiltonian

$$H(\theta, I; \tau) = \frac{I^2}{2} + V(\theta) \sum_{j=-\infty}^{+\infty} \delta(\tau - jT)\,, \tag{1}$$

where (I, θ) are conjugate action-angle variables ($0 \leq \theta < 2\pi$), with the usual quantization rules, $\theta \to \theta$ and $I \to I = -i\partial/\partial\theta$ (we set $\hbar = 1$) and $V(\theta) = -k(\theta - \pi)^2/2$. This Hamiltonian is the sum of two terms, $H(\theta, I; \tau) = H_0(I) + H_k(\theta; \tau)$, where $H_0(I) = I^2/2$ is the Hamiltonian of a particle freely moving on a circle parameterized by the coordinate θ, while $H_k(\theta; \tau) = V(\theta) \sum_j \delta(\tau - jT)$ represents a force acting on the particle and switched on and off instantaneously (kicking potential) at time intervals

Preprints (www.preprints.org) | NOT PEER-REVIEWED | Posted: 5 April 2021 doi:10.20944/preprints202104.0112.v1

T. The evolution from time tT^- (prior to the t-th kick) to time $(t+1)T^-$ (prior to the $(t+1)$-th kick) is described by a unitary operator U acting on the wave function ψ:

$$\begin{aligned} \psi_{t+1} &= U\,\psi_t = U_T U_k\,\psi_t\,; \\ U_T &= e^{-iTI^2/2}\,,\;\; U_k = e^{ik(\theta-\pi)^2/2}\,. \end{aligned} \tag{2}$$

This map is known as quantum sawtooth map, since the force $F(\theta) = -dV(\theta)/d\theta = k(\theta-\pi)$ has a sawtooth shape, with a discontinuity at $\theta = 0$.

Map (2) can be efficiently simulated on a quantum computer. The quantum algorithm simulating the sawtooth map dynamics is based on the forward/backward quantum Fourier transform between action (momentum) and angle bases. Such an approach is convenient since the operator U, introduced in Eq. (2), is the product of two operators, U_k and U_T, diagonal in the θ and I representations, respectively. This quantum algorithm requires the following steps for one map iteration:

- We apply U_k to the wave function $\psi(\theta)$. In order to decompose the operator U_k into one- and two-qubit gates, we first of all write θ in binary notation:

$$\theta = 2\pi \sum_{j=1}^{n} \alpha_j 2^{-j}\,, \tag{3}$$

with $\alpha_i \in \{0,1\}$. As n is the number of qubits, the total number of levels in the quantum sawtooth map is $N = 2^n$. Using expansion (3), we can decompose U_k into a product of n^2 two-qubit operations, each acting non-trivially only on the qubits j_1 and j_2. In the computational basis $\{|\alpha_{j_1}\alpha_{j_2}\rangle\}$ each two-qubit gate can be written as $\exp(i2\pi^2 k D_{j_1,j_2})$, where D_{j_1,j_2} is a diagonal matrix:

$$D_{j_1,j_2} = \begin{bmatrix} \frac{1}{4n^2} & 0 & 0 & 0 \\ 0 & -\frac{1}{2n}\left(\frac{1}{2^{j_1}} - \frac{1}{2n}\right) & 0 & 0 \\ 0 & 0 & -\frac{1}{2n}\left(\frac{1}{2^{j_2}} - \frac{1}{2n}\right) & 0 \\ 0 & 0 & 0 & \left(\frac{1}{2^{j_1}} - \frac{1}{2n}\right)\left(\frac{1}{2^{j_2}} - \frac{1}{2n}\right) \end{bmatrix}. \tag{4}$$

Neglecting a global phase factor of no physical significance, we can decompose $\exp(i2\pi^2 k D_{j_1,j_2})$ in terms of quantum gates (P and CP) available in the IBM Qiskit interface:

$$e^{i2\pi^2 k D_{j_1,j_2}} = \begin{pmatrix} 1 & 0 & 0 & 0 \\ 0 & e^{-\frac{i\pi^2 k}{2^{j_1} n}} & 0 & 0 \\ 0 & 0 & 1 & 0 \\ 0 & 0 & 0 & e^{-\frac{i\pi^2 k}{2^{j_1} n}} \end{pmatrix} \begin{pmatrix} 1 & 0 & 0 & 0 \\ 0 & 1 & 0 & 0 \\ 0 & 0 & e^{-\frac{i\pi^2 k}{2^{j_2} n}} & 0 \\ 0 & 0 & 0 & e^{-\frac{i\pi^2 k}{2^{j_2} n}} \end{pmatrix} \begin{pmatrix} 1 & 0 & 0 & 0 \\ 0 & 1 & 0 & 0 \\ 0 & 0 & 1 & 0 \\ 0 & 0 & 0 & e^{\frac{i\pi^2 k}{2^{j_1+j_2-1}}} \end{pmatrix}. \tag{5}$$

The first two factors in the product correspond to phase-shift gates (P gates) applied to qubit j_1 and j_2, respectively, while the last one corresponds to a controlled phase-shift gate (CP gates) applied on both qubits, if $j_1 \neq j_2$, and to a P gate if $j_1 = j_2$. Overall we need then $n^2 - n$ CP e $2n^2 + n$ P gates to implement U_k. As U_k is the product of diagonal matrices in the θ representation, the order of P and CP gates is irrelevant. Therefore, changing their order allows combining gates applied to the same qubits, thus improving the efficiency of the quantum algorithm. We then reduce the number of quantum gates needed to implement U_k to $n(n-1)/2$ CP and n P gates.
- The change from the θ to the I representation is obtained by means of the quantum Fourier transform (QFT), which requires n Hadamard (H) gates and $\frac{1}{2}n(n-1)$ CP gates. The correct order of qubits after the Fourier transform is obtained by simply relabeling qubits, thus avoiding $\lfloor n/2 \rfloor$ physical SWAP gates.

Preprints (www.preprints.org) | NOT PEER-REVIEWED | Posted: 5 April 2021 doi:10.20944/preprints202104.0112.v1

- In the I representation, the operator U_T has essentially the same form as the operator U_k in the θ representation and can therefore be similarly decomposed.
- We return to the initial θ representation by application of the inverse QFT.

Overall, this quantum algorithm requires $O(n^2)$ gates per map iteration. This number is to be compared with the $O(n2^n)$ operations required by a classical computer to simulate one map iteration using the fast Fourier transform. The quantum simulation of the quantum sawtooth map dynamics is then exponentially faster than any known classical algorithm. Note that the resources required to the quantum computer to simulate the sawtooth map are only logarithmic in the system size N. With the above discussed improvements of the quantum circuit, we need $2(n^2 - n)$ CP, $2n$ P, and $2n$ H gates to simulate one step of the quantum sawtooth map. Which corresponds to 24 quantum gates (12 single-qubit a 12 two-qubit gates) for the case $n = 3$ which we have simulated on the IBM quantum hardware.

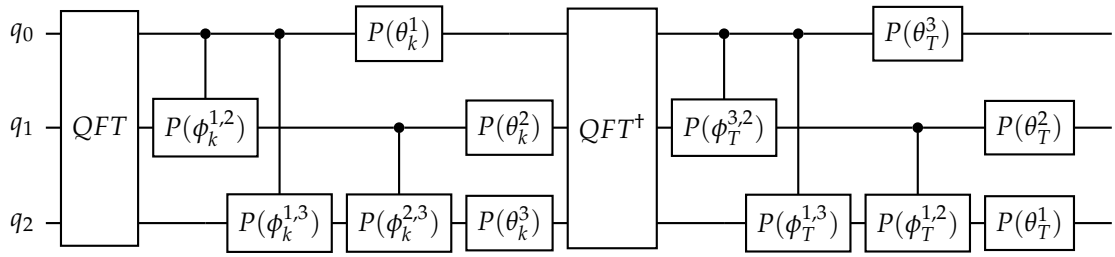

Figure 1. *Quantum circuit of sawtooth map with $n = 3$. The angles used in the P gates are obtained by changing order of the gates and combining them. The explicit formulas for the angles are given as the following: $\theta_k^j = -\frac{2\pi^2 k}{2^j} + \frac{\pi^2 k}{2^{2j-1}}$, $\theta_T^j = \frac{2N^2T}{2^{j+2}} - \frac{N^2T}{2^{2j+1}}$, $\phi_k^{j_1,j_2} = \frac{2\pi^2 k}{2^{j_1+j_2-1}}$, $\phi_T^{j_1,j_2} = -\frac{2N^2T}{2^{j_1+j_2+1}}$. The circuit avoids SWAP gates via relabeling of qubits after the QFT and the inverse QFT.*

2.2. Dynamical localization for the sawtooth map

The classical limit of the quantum sawtooth map is obtained for $k \to \infty$ and $T \to 0$, at constant $K = kT$. The classical motion is chaotic for $K < -4$ and $K > 0$. Although the sawtooth map is a deterministic system, in this regime the motion along the momentum direction is in practice indistinguishable from a random walk, with diffusion in the momentum variable. If we consider a classical ensemble of trajectories with fixed initial momentum m_0 and random initial angle θ, the second moment of the distribution grows linearly with the number t of map iterations,

$$\langle (\Delta m)^2 \rangle \approx Dt, \tag{6}$$

with the diffusion coefficient $D(k) \approx (\pi^2/3)k^2$ for $K > 1$.

The quantum sawtooth map, in agreement with the correspondence principle, initially exhibits diffusive behavior, with the classical diffusion coefficient D. However, after a break time $t^\star$, quantum interference leads to suppression of diffusion. For $t > t^\star$ the quantum distribution reaches a steady state which decays exponentially over the momentum eigenbasis:

$$W_m \equiv \left| \langle m|\psi \rangle \right|^2 \approx \frac{1}{\ell} \exp\left[-\frac{2|m - m_0|}{\ell} \right], \tag{7}$$

where the index m singles out the momentum eigenstates ($I|m\rangle = m|m\rangle$) and the system is initially prepared in the eigenstate $|m_0\rangle$. Therefore, for $t > t^\star$ only

$$\sqrt{\langle (\Delta m)^2 \rangle} \approx \sqrt{Dt^\star} \approx \ell \tag{8}$$

levels are populated.

Preprints (www.preprints.org) | NOT PEER-REVIEWED | Posted: 5 April 2021 doi:10.20944/preprints202104.0112.v1

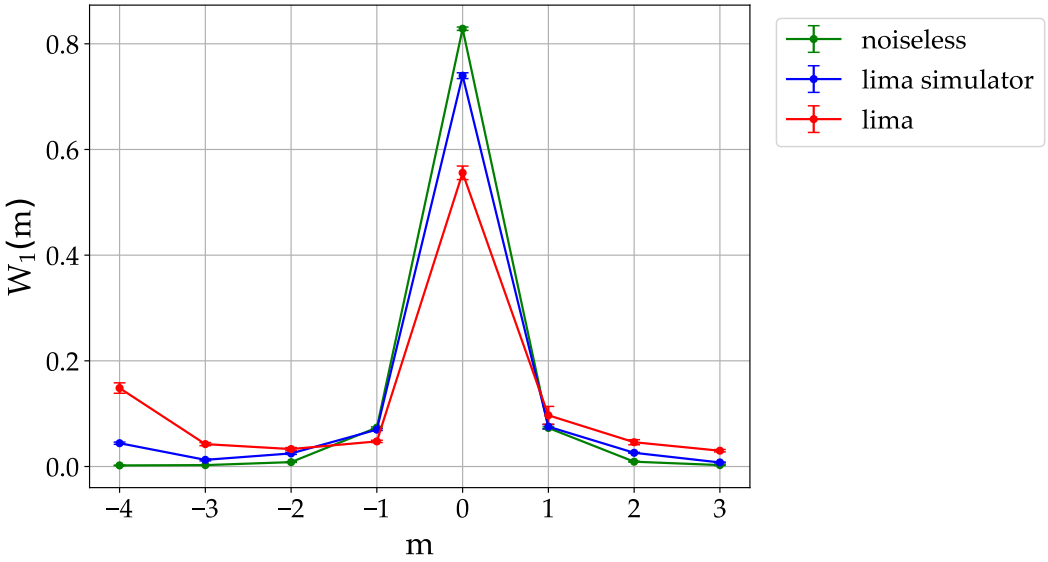

Figure 2. Dynamical localization in the quantum sawtooth map with $n = 3$ qubits, $K = 1.5$, $k \approx 0.273$ ($T = 2\pi L/N$, with $L = 7$). Hereafter data from the quantum processors (here *lima*) are obtained after averaging over 10 repetitions of 8192 experimental runs. Data taken on February 26th, 2021.

An estimate of $t^\star$ and ℓ can be obtained by means of a heuristic argument [28]. Since the number of levels involved grows diffusively, $\propto \sqrt{t}$, and, due to the Heisenberg principle, the discreteness of levels is resolved down to an energy spacing $\propto 1/t$, then the discreteness of spectrum eventually dominates. The localized wavefunction has significant projection over about ℓ eigenstates of the Floquet operator U, which determines the evolution of the system over one map step. This operator is unitary and therefore its eigenvalues can be written as $\exp(i\lambda_i)$, with λ_i (known as quasienergies) distributed in the interval $[0, 2\pi[$. The mean level spacing between quasienergy eigenstates which significantly determine the dynamics is $\Delta E \approx 2\pi/\ell$. The Heisenberg principle tells us that the minimum time required to the dynamics to resolve this energy spacing is given by

$$t^\star \approx 1/\Delta E \approx \ell. \tag{9}$$

Relations (8) and (9) imply

$$t^\star \approx \ell \approx D. \tag{10}$$

The quantum localization can be detected if ℓ is smaller than the system size N.

3. Quantum computing of dynamical localization

We simulate dynamical localization with $n = 3$ qubits on a real quantum hardware. The initial condition is peaked in momentum, $\psi_0(m) = \delta_{m,m_0}$, with $m_0 = 0$. The quantum algorithm for the sawtooth map allows us to compute the wave vector $\psi_t(m)$ as a function of the number of map steps, and then the momentum probability distribution $W_t(m) = |\psi_t(m)|^2$. We consider $k \approx 0.273 < 1$, so that the distribution is already localized after a single map step. On the other hand, we use $K = 1.5$, corresponding to diffusive behavior for the underlying classical dynamics. In Figure 2 we compare after $t = 1$ map step the ideal, noiseless distribution (green curve) with the Qiskit simulator (blue curve), used to test the quantum algorithm before submitting it to a real quantum hardware (red curve). Data for the quantum hardware are for the recently released (January 8th, 2021) *lima* quantum processor. This machine has a nominal quantum volume $V_Q = 8$ (i.e., a single number meant to encapsulate the quantum computer performance [29]), which is equal or smaller than the quantum

Preprints (www.preprints.org) | NOT PEER-REVIEWED | Posted: 5 April 2021 doi:10.20944/preprints202104.0112.v1

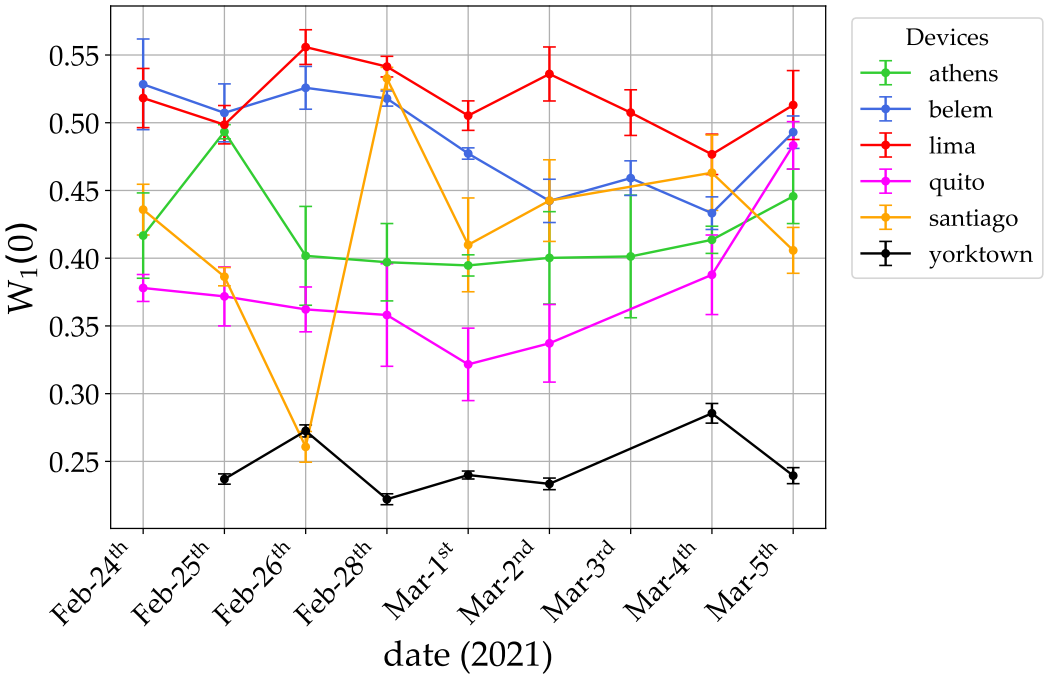

Figure 3. Height of the localization peak after one map step for several quantum processors. Data taken from February 24th to March 5th, 2021.

volume of other freely available quantum processors. Nevertheless, in our simulation we obtained the best results for the localization problem with this machine (see discussion below).

As we can see in Figure 2, the quantum hardware exhibits a localization peak after a single map step. On the other hand, the height of the peak, $W_1(0) \approx 0.56$, is significantly smaller than the noiseless value, $W_1(0) \approx 0.83$, and the prediction of the Qiskit simulator, $W_1(0) \approx 0.74$. These results show that the Qiskit simulator is too simplified, that is, it does not include all the relevant noise channels. It is also interesting to remark that, while the ideal distribution is symmetric around its peak, the noisy ones are markedly asymmetric. We interpret this asymmetry as a consequence of the binary coding of momentum eigenstate. For instance, a noise channel leading to a flipping of the most significant qubit would induce a probability transfer from the peak ($m = 0$, corresponding to the state $|100\rangle$ of the three qubits) to the state $|000\rangle$ (corresponding to $m = -4$).

To compare the performance of different freely available quantum machines, we ran the sawtooth quantum algorithm for one map step for several days (from February 24th to March 5th, 2021). Data are for *lima*, *belem* and *quito* (relase date January 8th, 2021, quantum volume $V_Q = 16$), *santiago* (June 3rd, 2020, $V_Q = 32$), *athens* (March 3rd, 2020, $V_Q = 32$), and *ibmqx2 - yorktown* (January 24th, 2017, $V_Q = 8$). This latter is an old machine having a low quantum volume, but its bow-tie layout is in principle more favorable for the present application, as it allows direct connectivity between all the three qubits involved in the algorithm. Comparing the height of the localization peak for several days, we can conclude that *lima* is the machine performing better, both in terms of the best achieved performance ($W_1(0) \approx 0.56$) and of constancy of the obtained results.

To further test the capabilities of quantum processors to simulate dynamical localization, in Figure 4 we show the peak value as a function of the number of kicks. For the noiseless case the distribution remains localized with fluctuations of $W_t(0)$ around 0.9. For the *ibmqx2 - yorktown* quantum processor the peak at $m = 0$ does not emerge from noise already at $t = 2$. On the other hand, for the *lima* quantum processor the peak is visible up to $t = 3$ kicks. The Qiskit simulator underestimates noise and predicts a decay of the peak in $3 - 5$ map steps (for *ibmx2 - yorktown*) and in $10 - 15$ kicks for *lima*. Overall, the data of Figs. 3 and 4 testify the significant improvement of quantum hardware performance in the last few years.

Preprints (www.preprints.org) | NOT PEER-REVIEWED | Posted: 5 April 2021 doi:10.20944/preprints202104.0112.v1

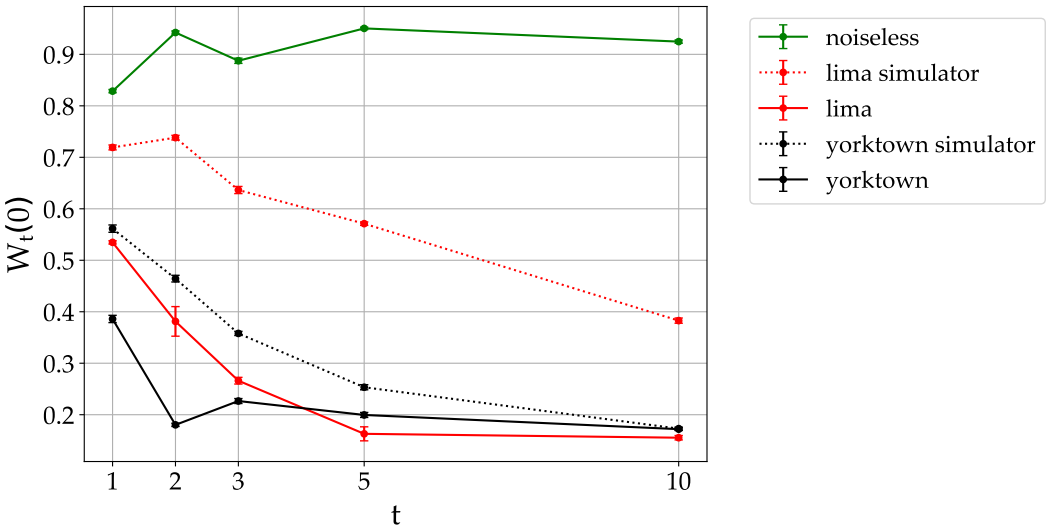

Figure 4. Height of the localization peak as a function of the number of map steps, for parameter values as in Fig. 2. Data are for *lima* (red) and *ibmqx2 - yorktown* (black). Data taken on February 14th (*ibmqx2 - yorktown*) and March 5th, 2021 (*lima*).

4. Conclusions

We have simulated the dynamical localization phenomenon of the quantum sawtooth map by means of several freely available IBM quantum processors, remotely accessed through cloud quantum programming. The localization peak emerges from noise, even though significantly reduced with respect to the noiseless dynamics, with up to three steps of the sawtooth map model for three qubits. Our results demonstrate a significant improvement of the performances of the available quantum processors over the past few years. This study shows that quantum computing of dynamical localization may be employed as a fast and convenient benchmark to check the performance of future generations of quantum processors. In particular, we could envision studying the maximum number n of qubits for which the peak height after one kick is reproduced with a given accuracy. Since the number of elementary quantum gates required to simulate one map step scales as n^2, in this "localization test" both the number of qubits and the circuit depth grow with n. The results of this work show that, for $n = 3$, the localization test does not necessarily agree with the quantum volume measure.

Author Contributions: A.P. and S. Y. C. performed quantum simulations by coding actual IBM quantum processors. G.B. supervised the work and drafted the manuscript. All authors discussed the results and contributed to revision of the manuscript.

Funding: S.M. acknowledges support by the Italian PRIN 2017, the Fondazione CARIPARO, and the Horizon 2020 research and innovation programme under grant agreement No 817482 (Quantum Flagship - PASQuanS). D.G. acknowledges the Italian Ministry of Education, University and Research (MIUR): "Dipartimenti di Eccellenza Program (2018-2022)", Department of Physics, University of Pavia. G.B. acknowlewdges the financial support of the INFN through the project QUANTUM.

Acknowledgments: We acknowledge use of the IBM Quantum Experience for this work. The views expressed are those of the authors and do not reflect the official policy or position of IBM company or the IBM-Q team. F. Tacchino is gratefully acknowledged for co-supervising the work of S.-Y. Chang during her visit at the University of Pavia in July 2019.

Conflicts of Interest: The authors declare no conflict of interest. The funders had no role in the design of the study; in the collection, analyses, or interpretation of data; in the writing of the manuscript, or in the decision to publish the results.

Preprints (www.preprints.org) | NOT PEER-REVIEWED | Posted: 5 April 2021 doi:10.20944/preprints202104.0112.v1

References

1. Benenti, G., Casati, G., Rossini, D., and Strini, G. *Principles of quantum computation and information (A comprehensive textbook)*; World Scientific, Singapore, 2019.
2. Feynman, R. P. Simulating Physics with Computers. *Int. J. Theor. Phys.* **1982**, *21*, 467.
3. Lloyd, S. Universal quantum simulators. *Science* **1996**, *273*, 1073.
4. Abrams, D. and Lloyd, S. Simulation of many-body Fermi systems on a universal quantum computer. *Phys. Rev. Lett.* **1997**, *79*, 2586.
5. Zalka, C. Efficient simulation of quantum systems by quantum computers. *Fortschr. Phys.* **1998**, *46*, 877.
6. Schack, R. Using a quantum computer to investigate quantum chaos. *Phys. Rev. A* **1998**, *57*, 1634
7. Terhal, B. M. and DiVincenzo, D. P. Problem of equilibration and the computation of correlation functions on a quantum computer. *Phys. Rev. A* **2000**, *61*, 022301.
8. Ortiz, G., Gubernatis, J. E., Knill, E., and Laflamme, R., *Phys.Rev. A* **2001**, *64*, 022319.
9. Georgeot, B. and Shepelyansky, D. L. Exponential gain in quantum computing of quantum chaos and localization. *Phys. Rev. Lett.* **2001**, *86*, 2890.
10. Benenti, G. and Strini, G. Quantum simulation of the single-particle Schrodinger equation. *Am. J. Phys.* **2008**, *76*, 657.
11. Georgescu, I. M., Ashhab, S., and Nori, F. Quantum simulation. *Rev. Mod. Phys.* **2014**, *86*, 153.
12. Chiesa A., Tacchino F., Grossi M., Santini P., Tavernelli I., Gerace D., and Carretta S., Quantum hardware simulating four-dimensional inelastic neutron scattering, *Nat. Phys.* **2019**, *15*, 455.
13. Tacchino, F., Chiesa A., Carretta, S., and Gerace, D. Quantum computers as universal quantum simulators: State-of-the-art and perspectives, *Adv. Quantum Technol.* **2020**, *3*, 190052.
14. Arute, F. *et al.* Quantum supremacy using a programmable superconducting processor. *Nature* **2019**, *574*, 505.
15. Zhong, H. S. *et al.* Quantum computational advantage using photons. *Science* **2020**, *370*, 1460.
16. Zhou, Y., Stoudenmire, E. M., and Waintal, X. What Limits the Simulation of Quantum Computers? *Phys. Rev. X* **2020**, *10*, 041038.
17. Casati, G., Chirikov, B. V., Ford, J., and Izrailev, F.M. Stochastic behavior of a quantum pendulum under a periodic perturbation. *Lecture Notes in Physics* **1979**, *93*, 334.
18. Izrailev, F. M. Simple models of quantum chaos:spectrum and eigenfunctions. *Phys. Rep.* **1990**, *196*, 299.
19. Koch, P. M. and van Leeuwen, K. A. H. The importance of resonances in microwave "ionization" of excited hydrogen atoms. *Phys. Rep.* **1995**, *255*, 289.
20. Moore, F. L., Robinson J. C., Barucha, C. F., Sundaram, B., and Raizen, M. G. Atom optics realization of the quantum delta-kicked rotor. *Phys. Rev. Lett.* **1995**, *75*, 4598.
21. Chabé, J., Lemarié, G., Grémaud, B., Delande, D., Szriftgiser, P., and Garreau, J. C. Experimental Observation of the Anderson Metal-Insulator Transition with Atomic Matter Waves. *Phys. Rev. Lett.* **2008**, *101*, 255702.
22. Manai. I., Clément, J.-F., Chicireanu, R., Hainaut, C., Garreau, J. C., Szriftgiser, P., and Delande, D. Experimental Observation of Two-Dimensional Anderson Localization with the Atomic Kicked Rotor. *Phys. Rev. Lett.* **2015**, *115*, 240603.
23. Henry, M. K., Emerson, J., Martinez, R., and Cory, D. G. Study of localization in the quantum sawtooth map emulated on a quantum information processor. *Phys. Rev. A* **2006**, *74*, 062317.
24. Fishman, S., Grempel, D. R., and Prange, R. E. Chaos, Quantum Recurrences, and Anderson Localization. *Phys. Rev. Lett.* **1982**, *49*, 509.
25. Montangero, S. Dynamically localized systems: Exponential sensitivity of entanglement and efficient quantum simulations. *Phys. Rev. A* **2004**, *70*, 032311.
26. Benenti, G., Casati, G., Montangero, S., and Shepelyansky, D. L. Efficient quantum computing of complex dynamics. *Phys. Rev. Lett.* **2001**, *87*, 227901.
27. Benenti, G., Casati, G., Montangero, S., and Shepelyansky, D. L. Dynamical localization simulated on a few-qubit quantum computer. *Phys. Rev. A* **2003**, *67*, 052312.
28. Chirikov, B. V., Izrailev, F. M., and Shepelyansky, D. L. Dynamical stochasticity in classical and quantum mechanics. *Sov. Sci. Rev. C* **1981**, *2*, 209.
29. Cross A. W., Bishop L. S., Sheldon S., Nation, P. D., and Gambetta J. M., Validating quantum computers using randomized model circuits, *Phys. Rev. A* **2019**, *100*, 032328.

Preprints (www.preprints.org) | NOT PEER-REVIEWED | Posted: 5 April 2021 doi:10.20944/preprints202104.0112.v1